Potential Contributions of Airborne Radio Occultation Observations to Forecast Improvement of Hurricanes and Atmospheric Rivers

J.S. Haase[1], M.J. Murphy Jr. [1], B. Cao[1], S.-H. Chen[2], M. Zheng[3], F.M. Ralph[3], B. J. Murphy[4], X.-M. Chen[2], K.-N. Wang[1], S.-Y. Chen[5], C. Y. Huang[5], J.L. Garrison[4]
[1]UC San Diego; [2]UC Davis; [3]CW3E UC San Diego; [4]Purdue University; [5]Central Taiwan University

Airborne Radio Occultation (ARO)

$$N = (n-1)\cdot 10^6 = k_1\frac{P}{T} + k_2'\frac{e}{T^2}$$

- Measures GNSS signal propagation delay from satellites below the horizon
- Refractivity at tangent point is a function of pressure, temperature, water vapor pressure
- High vertical resolution
- Complementary to dropsondes
- Samples to the side of the flight track continuously, 25 per 7 hour flight

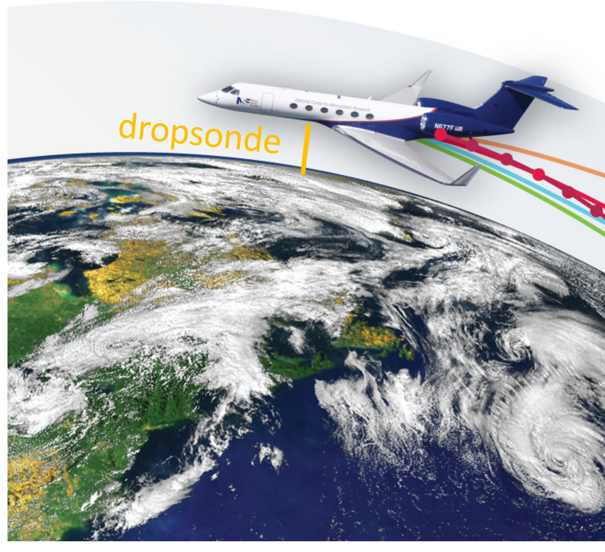

AR Recon 2018 Field campaign IOP1

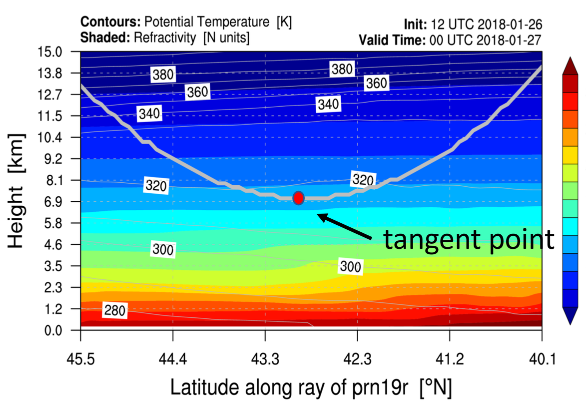

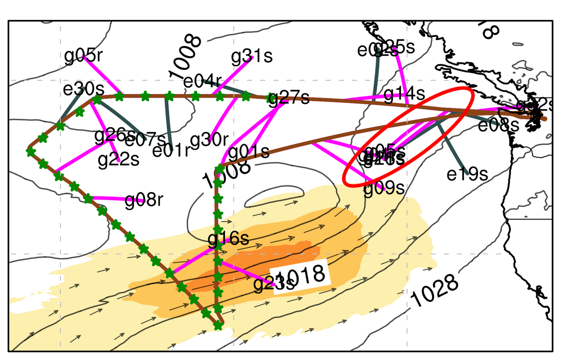

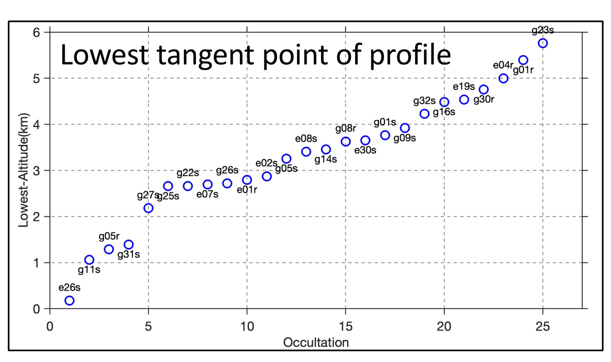

11/25 occultations penetrate below 3 km

Targeted observations

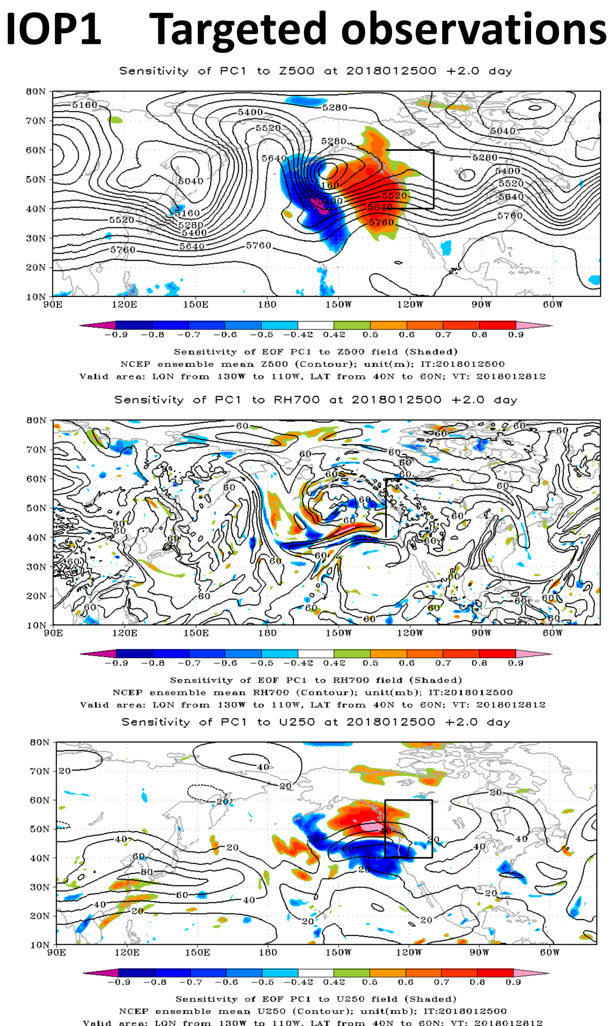

- ~7 hr flight.
- 17 GPS (14 Setting + 4 Rising).
- 8 Galileo (6 Setting +1 Rising).
- One Galileo occultation penetrates to the surface.
- Five rising occultations, one penetrates to 2 km.
- EXCEPTIONALLY GOOD FOR SIMPLE CLOSED-LOOP RECEIVER HARDWARE.

Dropsonde comparison for data quality evaluation

- Negligible difference between two independent receivers.
- 1% difference between two constellations GPS and Galileo.
- 2-3% difference with ECMWF model and dropsonde.
- Structural variations match very well.

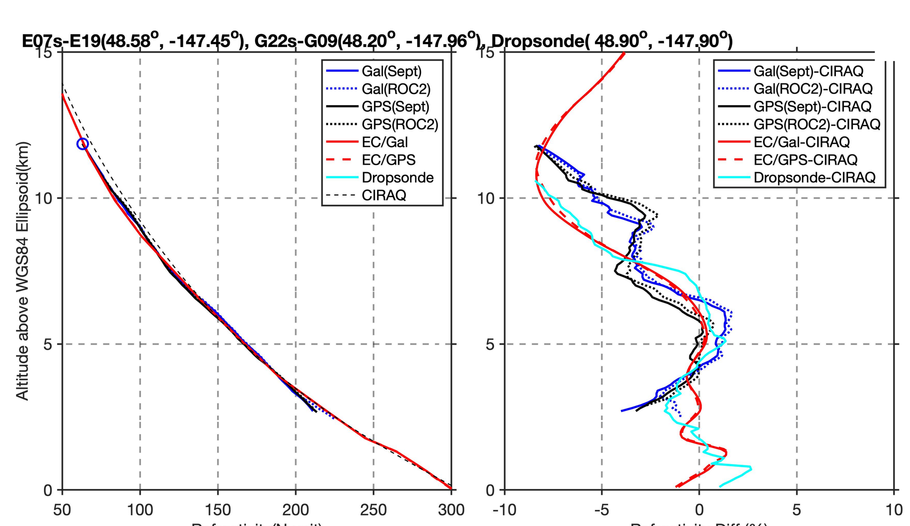

Spatial variations in temperature field sampled by ARO

WRF DROPS Temperature@ 7 km

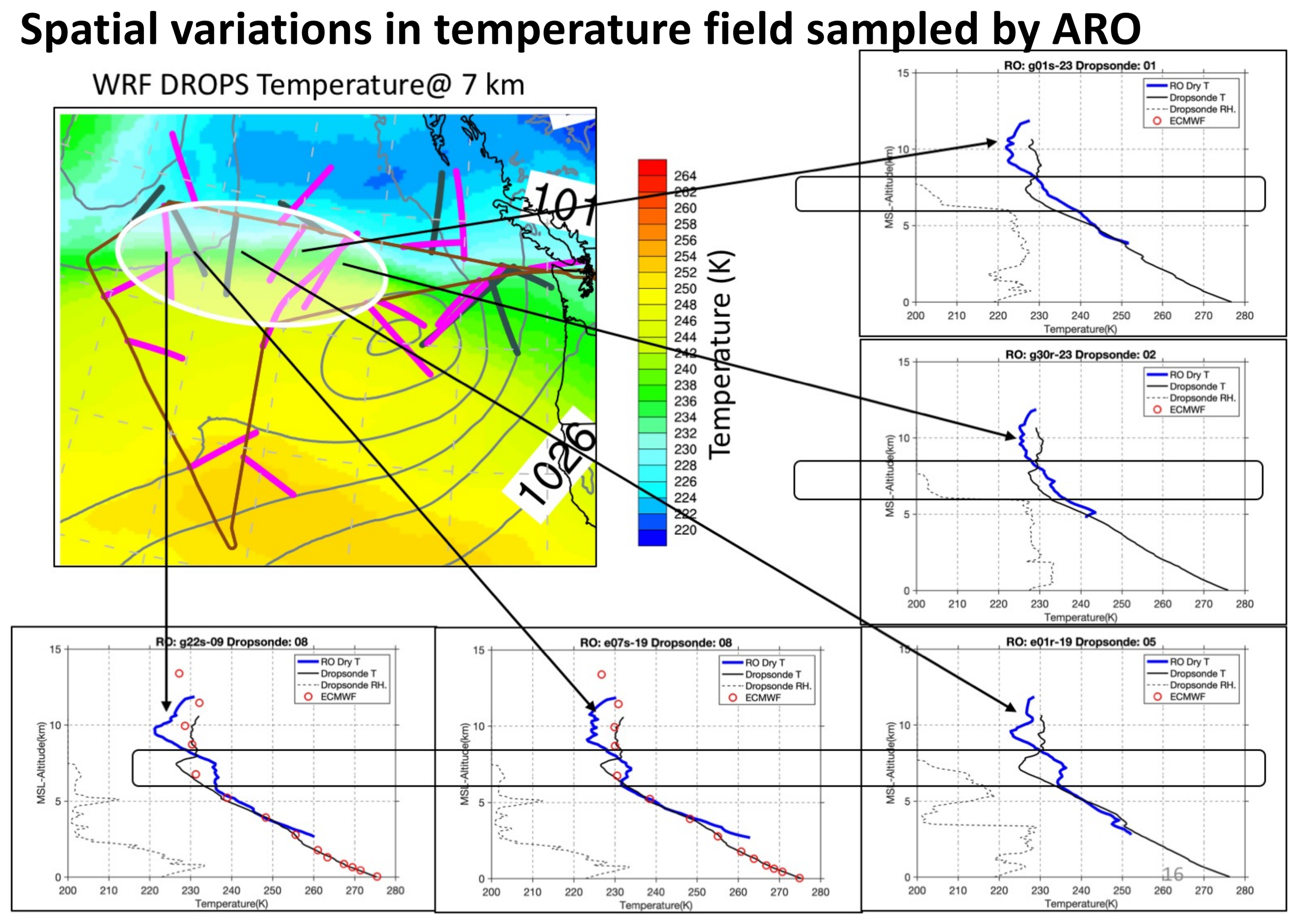

- Systematic fluctuations in temperature over the range from 6-11 km altitude correspond to strong temperature gradient in hi-res WRF model run that assimilates dropsondes.

Potential for deployment on commercial aircraft

Flights in GTS database in one day
~3500 occultations over CONUS
11 Sept 2013 CO extreme flooding event
(Chen 2017; Gochis et al., 2015)

14 transatlantic AMDAR flights in one day
~250 occultations (GPS only)
(Lesne et al., 2002)

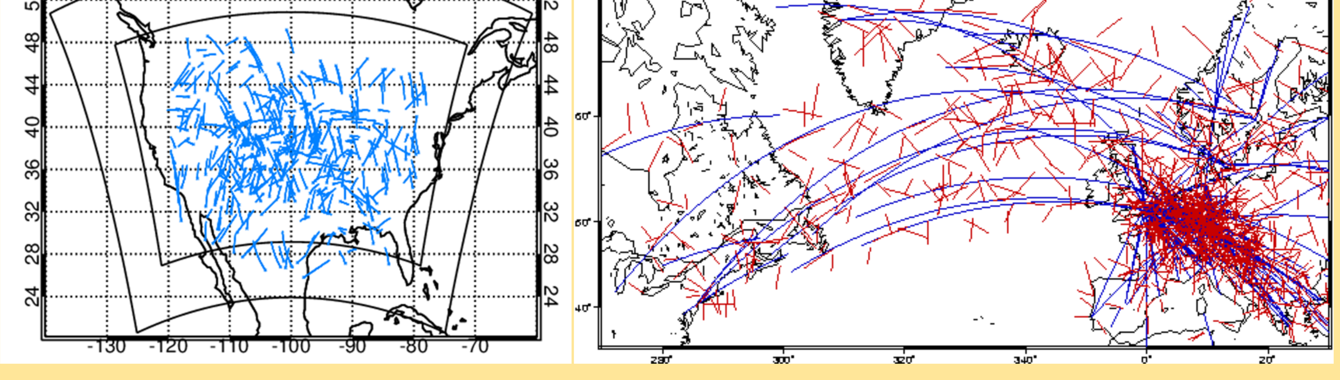

Data assimilation experiment

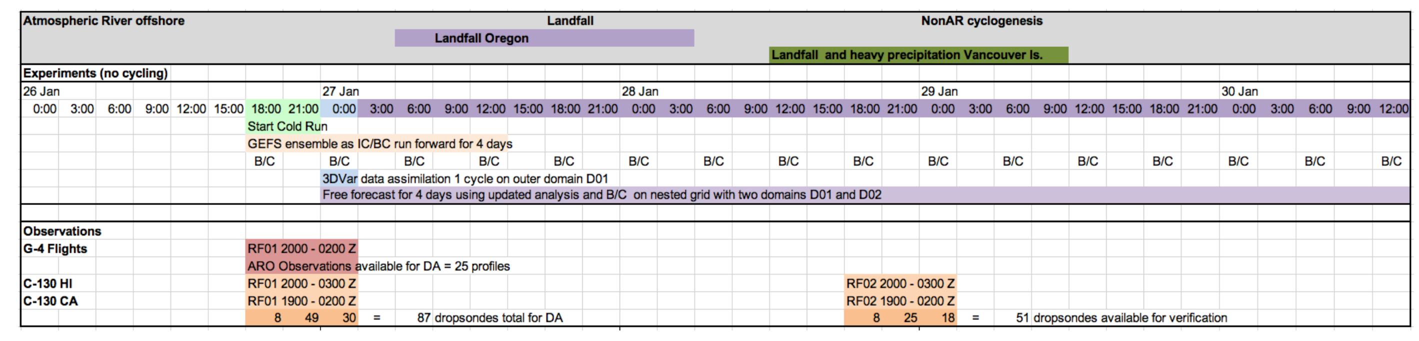

NODA	DROP	DROP_ARO
14.70	14.72	14.77
No Data Assimilation	GTS conventional data + dropsondes	GTS conventional data + dropsondes + ARO

Config 07.01 (GEFS forcing with Ensembles)		
	14.7X	
Description	two domains	
Forecast model	WRF-ARW V4.1	
DA System	WRFDA V4.1	
DA technique	3DVAR **No Cycling ASCII prepbufr**	
Initial/Bdry Conditi	GEFS Operational Forecast (from HAS 1.0 deg)	
# of ensembles	0 i.e. just the cntrl member (ens00)	
Domains	D01	D02
Assmilation	yes	no
Resolution	27 km	9 km
Mesh size	355 x 300	799 x 661
Nest feedbak	two way	two way
Model levels	48	
Model top	10 hPa	
Microphysics	Thompson (Double-Moment)	
Cumulus	Grell-Freitas	Grell-Freitas
PBL	YSU scheme	
Land Surface	Unified Noah land-surface model	
Longwave	RRTMG	
Shortwave	RRTMG	
Background Error	NMC method (24-12 hr fcsts)	
	15 Jan - 15 Feb 2018	
	intitalized at 00 & 12 UTC	
BE System	WRFDA GENBE V1.0	
	BE Covariance 5	

Data assimilation increment

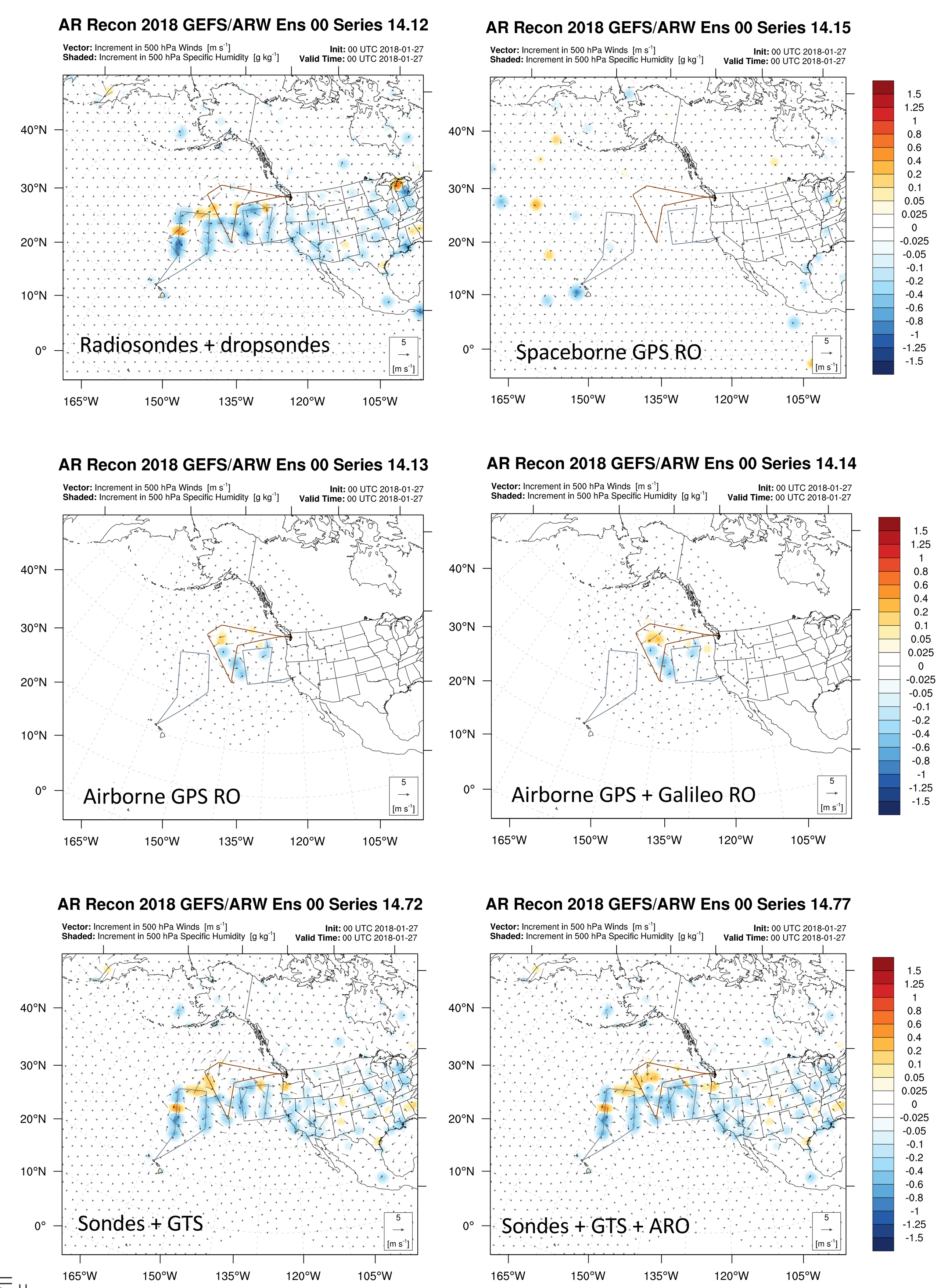

Impact on 12 hour forecast precipitation

Difference in Spec. Hum. Difference in precipitation

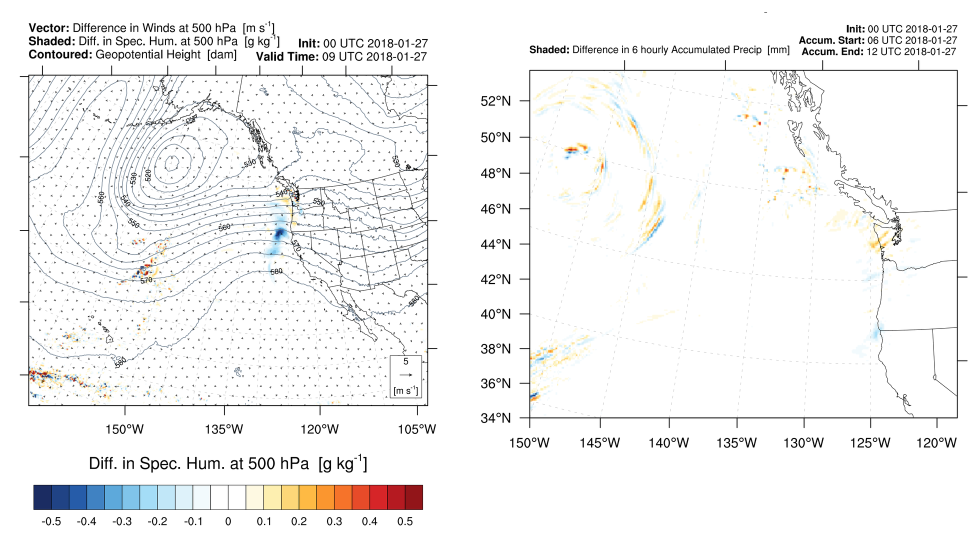

- ARO had an impact on the initial moisture fields that propagated downstream and affected precipitation at landfall.
- In this case, the precipitation was minor so the overall impact was minor.
- Perhaps sampling on 27 Jan at 18 Z upstream of the major precipitation at landfall on 28 Jan at 12 Z would show more impact.
- We can investigate more ways to use the forecast timing of the precipitation.
- The sensitivity of the PCA of precipitation to the observations may be a good predictor for this.

Hurricane Karl 2010 example case study

Experiments	Observations assimilated
CTRL	GTS + dropsondes
GDANn	CNTL + airborne RO non-drifting refractivity
GDAEd	CNTL + airborne RO excess phase w/drifting tangent points

Changes in the initial moisture, pressure, and vorticity fields

(GDAEd-CTRL) 3-km pressure and vorticity 1200 UTC 13 Sept. 2010

The vortex of the storm was more compact during early development, likely due to the increase in midlevel moisture and positive vorticity advection (right), compared to the CTRL experiment without ARO observations.

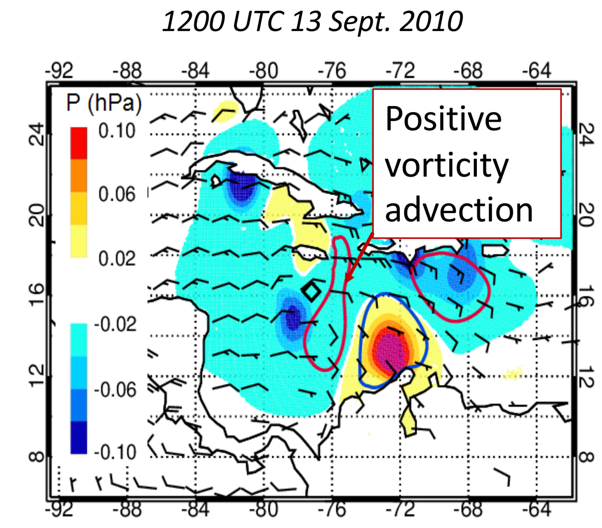

Importance of non-local DA operator

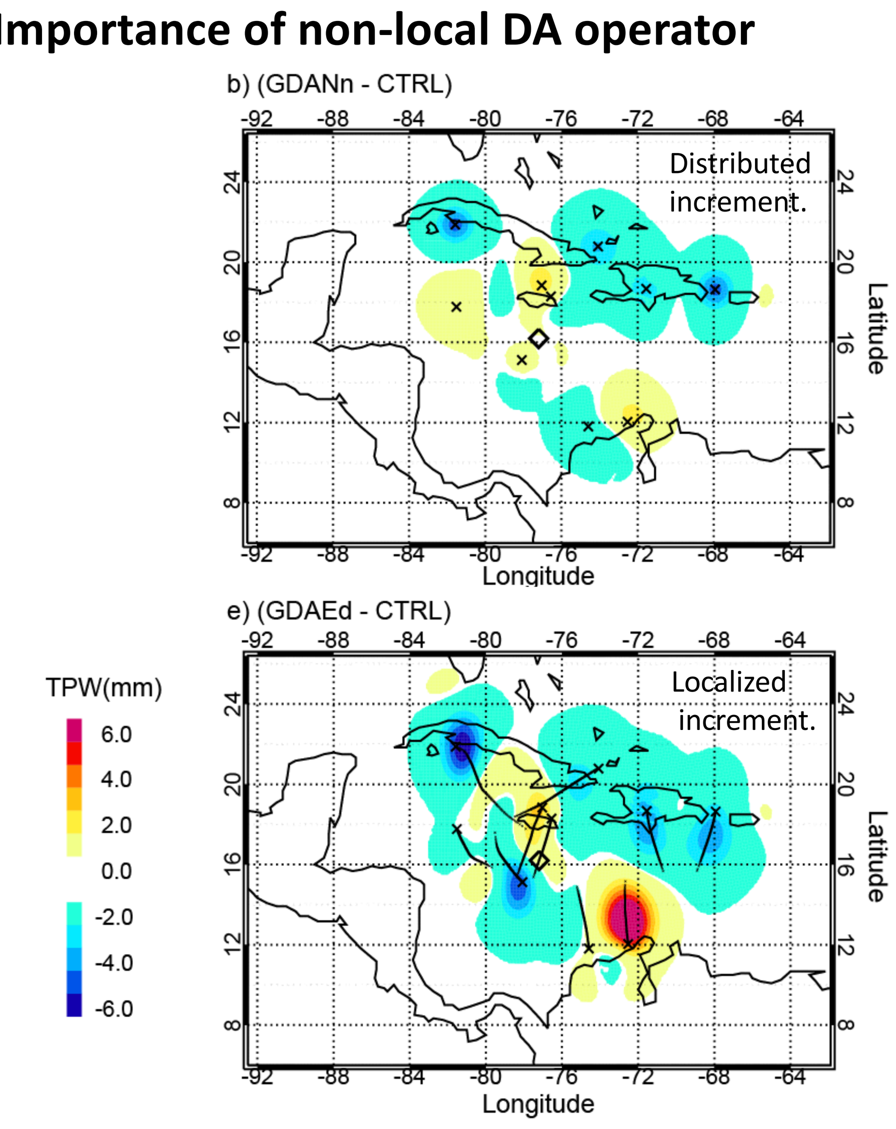

Impact on diabatic heating

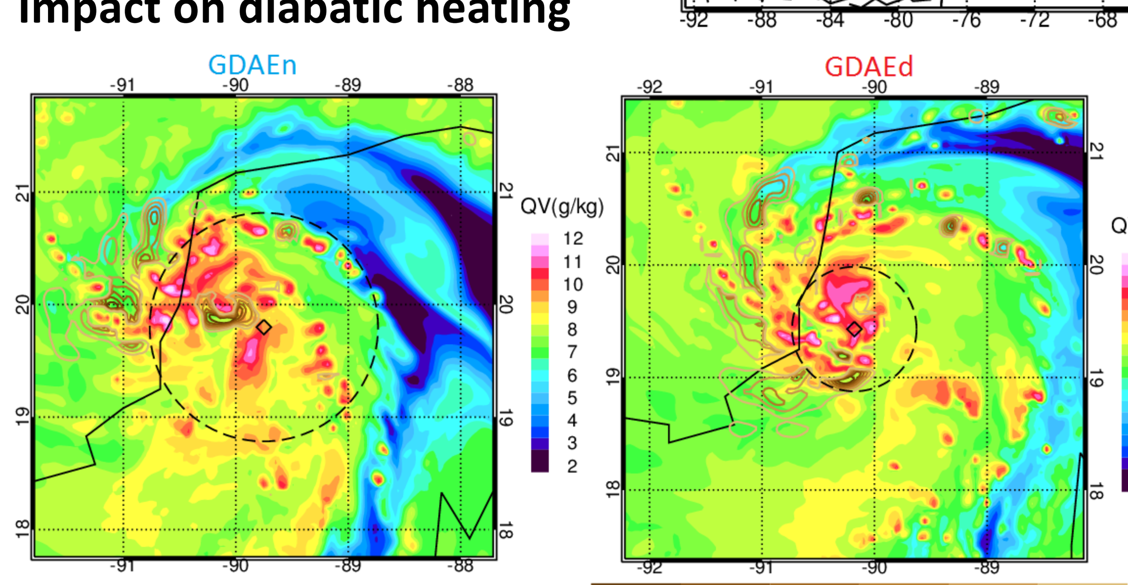

(left) Water vapor mixing ratio (color shading) and diabatic heating (brown contours) at 650 hPa at 0000 UTC 16 September of GDAEn and GDAEd. Areas of diabatic cooling ahead of the storm likely impeded the storm development.
Black diamonds indicate the position of the surface minimum sea level pressure of the simulated storm. Dashed circles indicate the radius of maximum 10-m wind.

Impact on hurricane intensity and track

Central sea level pressure Maximum 10-m wind

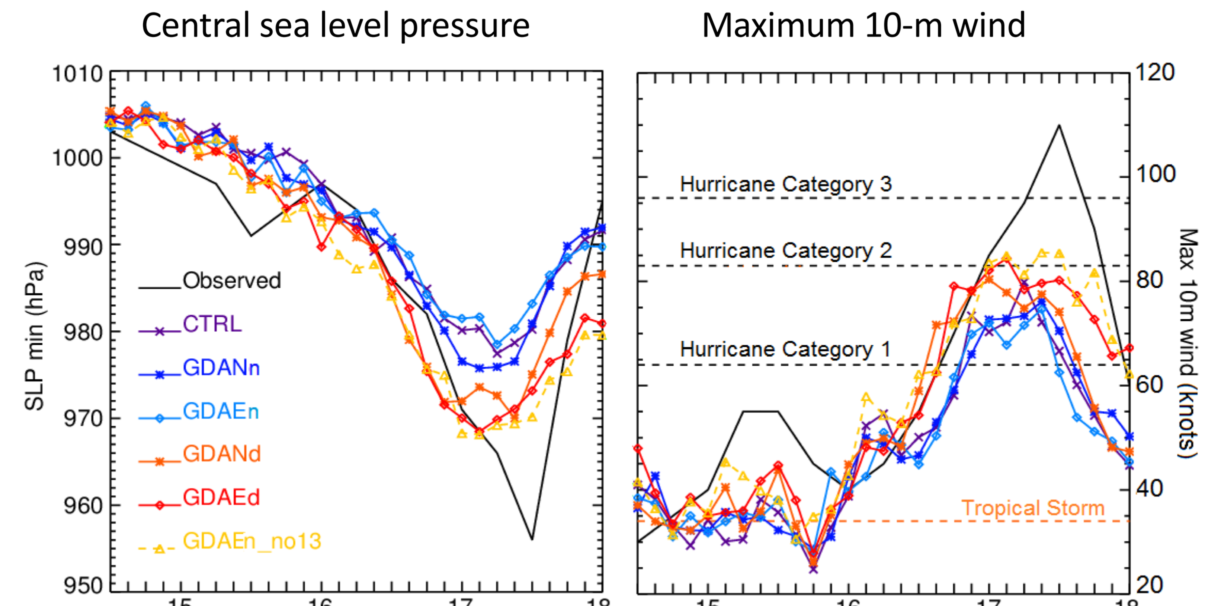

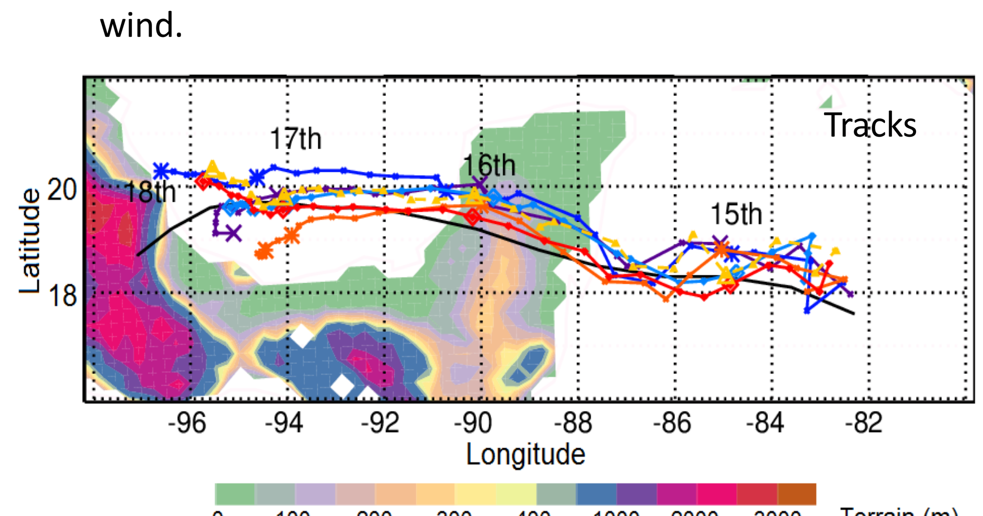

References
Chen, X. M., S. H. Chen, J. S. Haase, et al. (2018), The Impact of Airborne Radio Occultation Observations on the Simulation of Hurricane Karl (2010), *MWRv*, *146*, 329-350.
Chen, X. M. (2017), Airborne Radio Occultation Measurements and Their Impact on Severe Weather Prediction Using the Regional WRF Model, 132 pp, UC Davis, Davis, CA.
Haase, J. S., B. J. Murphy, P. Muradyan, F. Nievinski, K. M. Larson, J. L. Garrison, and K.-N. Wang (2014), First Results from an Airborne GPS Radio Occultation System for Atmospheric Profiling, *GeoRL*, *40*.
Lesne, O., J. Haase, G. Kirchengast, J. Ramsauer, and W. Poetzi (2002), Sensitivity analysis of GNSS radio occultation for airborne sounding of the troposphere, *Phys. and Chem. of the Earth*, *27*, 291-299.
Murphy, B. J., J. S. Haase, P. Muradyan, J. L. Garrison, and K.-N. Wang (2015), Airborne GPS radio occultation refractivity profiles observed in tropical storm environments, *JGR*, *120*, 1690-1790.
Wang, K. N., J. L. Garrison, J. S. Haase, and B. J. Murphy (2017), Improvements to GPS Airborne Radio Occultation in the Lower Troposphere Through Implementation of the Phase Matching Method, *JGR: Atmospheres*, *122*, 2017JD026568.

Acknowledgements
This work was supported by NSF GRANT 1642650, and NASA GRANT NNX15AU19G , NSF grants 100602-200912528, AGS 1015904, and AGS 1301835. We thank the CW3E AR Program and its sponsors, including the California Department of Water Resources, and the Army Corps of Engineers FIRO program. We thank NSF & the NCAR EOL facility for the loan of the Applanix navigation system, Adrian Borsa for the GNSS equipment loan, and Dave Jabson for his assistance with the ROC equipment. Flight time on the NOAA G-IV aircraft was provided by the National Oceanic and Atmospheric Administration. We would like to acknowledge the assistance of the NOAA Aircraft Operations Center staff, and in particular Gabriel DeFao and Jack Parrish.